ROMANIAN ACADEMY
School of Advanced Studies of the Romanian Academy
Institute of Biochemistry of the Romanian Academy

PHD THESIS SUMMARY

A novel strategy for inhibiting STAT3 activity using DNA minicircles in ovarian cancer

PHD COORDINATOR:
CSI Prof. Dr. Ștefan-Eugen Szedlacsek

PHD CANDIDATE:
Puiu Adina-Gabriela (Vasilescu)

2025

TABLE OF CONTENTS

I. INTRODUCTION

Signal Transducer and Activator of Transcription 3 (STAT3) is a transcription factor with a critical role in regulating cell growth, differentiation, survival and immune function (Timofeeva et al., 2012). Within the JAK/STAT3 signaling pathway, after stimulation of specific receptors, the Janus Kinase (JAK) proteins are activated and phosphorylate STAT3, determining its dimerization, activation and translocation to the nucleus (Bild, Turkson & Jove, 2002). Here, STAT3 binds specific response elements, such as gamma-activated sequence-like (GAS-like) motifs, located in the promoters of target genes (Ivashkiv & Donlin, 2014). The expression of these genes is thus modulated by STAT3, contributing to the control of the above-mentioned cell processes. Under normal physiological conditions, STAT3 activation is tightly controlled and transient (Timofeeva et al., 2012). However, persistent activation of STAT3 has been involved in the development and progression of several malignancies, including ovarian cancer. Its dysregulation can disrupt cellular homeostasis, contributing to unchecked proliferation, resistance to apoptosis and the creation of an immunosuppressive tumor microenvironment (TME) (Huang et al., 2000; Cheung, Leung & Wong, 2006; Davidson, Tropé & Reich, 2012; Jia et al., 2017). Ovarian cancer is recognized as one of the most severe gynecologic malignancies globally, owing to its silent progression and late-stage detection, with over 200,000 new cases annually (Ren et al., 2025). Therefore, a pressing need exists to develop novel target-specific therapeutic compounds against this malignancy. In the context of ovarian cancer, aberrant STAT3 signaling is particularly significant and is associated with poor prognosis, disease progression to advanced stages and resistance to chemotherapy, by upregulating proliferation and survival genes, such as *cyclin D1, c-myc, survivin, MCL1* (for myeloid cell leukemia-1), *PIM1* (for Pim-1 proto-oncogene, serine/threonine kinase), or *MMPs* (genes for matrix metalloproteinases), while suppressing apoptosis and enhancing angiogenesis (Huang et al., 2000; Wu et al., 2019). As a result, STAT3 is being actively explored as a therapeutic target, with various inhibitors under investigation aiming to disrupt its signaling in cancer and restore normal cellular function.

Efforts to inhibit STAT3 signaling have included inhibitors that target cytokines (e.g. IL-6) or cytokine receptors, like IL-6R, but did not show a significant effect on late-stage solid tumors and they can trigger collateral effects (Angevin et al., 2014; Goumas et al.,

2015; Baran et al., 2018). JAK inhibitors, even though some of them are already FDA-approved, exhibit pronounced systemic side effects (Qian, Xue & Shannon, 2022; Verstovsek et al., 2012). Peptides and small molecules targeting the STAT3 Src Homology 2 (SH2) domain (e.g., PYLKTK motif-containing inhibitor, or STATTIC, respectively) have also been used, yet these often suffer from low membrane permeability and insufficient efficacy, due to low affinity and specificity (Turkson et al., 2001; Schust et al., 2006). Nucleic acid-based approaches, including antisense oligonucleotides, which are meant to degrade the mRNA for STAT3, face challenges of instability and off-target effects despite their potential (Roth, 2005; Zhang et al., 2024). Decoy oligodeoxynucleotides (ODN-decoys) mimicking STAT3-binding sites and acting as competitors for the DNA-binding domain (DBD) of STAT3 have been studied in several types of cancer and they have shown promise *in vitro,* but were limited by rapid degradation *in vivo* (Gu et al., 2008; Sen et al., 2009, 2012; Souissi et al., 2011).

To address these limitations, we developed and characterized a small, double-stranded DNA minicircle (anti-STAT3 mcDNA) containing three GAS-like motifs to act as a stable decoy for STAT3. Furthermore, to address the unmet need for personalized therapy in ovarian cancer, we employed a novel design and validation strategy to create this molecule and utilized it here for the first time to inhibit STAT3 in ovarian cancer cells. As SKOV3 is the fifth-highest cell line in terms of STAT3 expression, it was chosen as our model for this disease (The Human Protein Atlas, 2025). We expect that this minicircle will effectively sequester STAT3, reduce target gene activation and inhibit proliferation while promoting apoptosis in SKOV3 ovarian cancer cells.

We consider that the developed minicircle offers several key advantages: (i) three GAS-like motifs on a single molecule, which enhances its probability of interacting with the DNA-binding domain of STAT3; (ii) the closed circular configuration that enhances molecular stability and protects against nuclease-mediated degradation; (iii) the likelihood of an extended half-life following *in vivo* administration and (iv) its simplicity, consisting of chemically unmodified DNA, which enables a cost-effective production. We expect these attributes to result in a significantly effective strategy to inhibit STAT3 activity in ovarian cancer, as well as in other STAT3-driven malignancies.

The present thesis is composed of a Theoretical Part and an Experimental Part. The Theoretical Part provides an overview of the universe of STAT proteins, with focus on STAT3, highlighting aspects as the structure, cellular functions, regulation and the

implications in disease that determined the choice to address the STAT3 protein in ovarian cancer as the subject of this thesis.

The Experimental Part represents the personal contribution of the author of this thesis. In this study, we report the design, validation, and *in vitro* evaluation of the anti-STAT3 mcDNA, as well as a mock minicircle control with scrambled GAS-like motifs, in SKOV3 ovarian cancer cells. First, we circularized precursor oligonucleotides through an enzymatic ligation method. The circularization was then validated through enzymatic restriction at specific sites and the binding specificity of the anti-STAT3 mcDNA to the STAT3 protein was evaluated through Electrophoretic Mobility Shift Assay (EMSA). In MTS assay, flow cytometry and Western blot experiments, we showed that anti-STAT3 mcDNA caused specific and remarkable inhibition, apoptosis and proliferation decrease of SKOV3 ovarian cancer cells with active STAT3. Additionally, quantitative PCR and Western blot demonstrated significant downregulation of anti-apoptotic and pro-survival genes *MCL1* and *PIM1* in anti-STAT3 mcDNA-treated SKOV3 cells, compared to the mock minicircle. All these results we obtained reveal the potential of anti-STAT3 mcDNA as a novel therapeutic strategy to inhibit STAT3 signaling in ovarian cancer. This strategy could also be explored in other STAT3-driven malignancies, pending further validation.

Hypothesis

The hypothesis of this PhD thesis is that a DNA minicircle targeting STAT3 will act as a decoy for the target protein, thus downregulating STAT3-modulated genes and causing inhibition, apoptosis and decreased proliferation in SKOV3 ovarian cancer cells.

Objectives of the thesis

- Design of a small, double-stranded DNA minicircle targeting the STAT3 protein
- Development of the DNA minicircle and validation of its structure
- Evaluation of the interaction between STAT3 and the DNA minicircle
- Inhibitory concentration determination of the DNA minicircle in model ovarian cancer cells
- Determination of DNA minicircle functional effects on representative ovarian cancer cells
- Evaluation of STAT3-modulated gene expression in a cell model for ovarian cancer, upon treatment with the DNA minicircle

II. THEORETICAL PART

1. STAT PROTEINS

The STAT family of proteins consists of seven members: STAT1, STAT2, STAT3, STAT4, STAT5A, STAT5B and STAT6, each of them being encoded by its corresponding gene. Despite their different localization, comparative sequence analysis and crystallography studies have shown that STAT proteins present a highly conserved structure (Becker, Groner & Müller, 1998; Calò et al., 2003). The molecular weights of the STAT proteins, depending on the member, range from 80 to 100 kDa (Hendry & John, 2004). STATs are 750-900 amino acid residues long and comprise six domains, each with a well-established role (Lim & Cao, 2006).

At the N-terminal end, all STAT proteins present an **N-terminal domain (NTD)**, which contains alpha helices and is very important for the interactions established with other transcription factors or cofactors, facilitating the dimerization process, in the presence or absence of phosphorylation (Strehlow & Schindler, 1998). The **coiled-coil domain (CCD)** is also called the all-helix domain, given the fact that it is a supercoil consisting of only alpha helices. Due to the presence of a nuclear localization signal (NLS), it is involved in those protein interactions necessary for nuclear import (Awasthi, Liongue & Ward, 2021). Next, the **DNA-binding domain (DBD)**, with an immunoglobulin-like fold, is crucial for the regulation that STAT proteins exert on target genes due to their primary function as transcription activators. Through this domain, STATs bind to the specific DNA motifs localized in the gene promoter. It has also been discovered that this domain has implications for nuclear import (Horvath, Wen & Darnell, 1995; Awasthi, Liongue & Ward, 2021). Further, the **linker domain (LD)** is a short one and provides the structural organization of the STAT protein during the activation phase and the DNA-binding phase, also being physically involved in the transcription complex formation (Yang et al., 1999). The **Src homology 2 domain (SH2 Domain)** recognizes and binds specific motifs containing phosphorylated tyrosines within receptor complexes. Also, upon its tyrosine phosphorylation, it functions as a contact point for homo- or heterodimerization of STAT proteins through their SH2 domains (Liu, Gaffen & Goldsmith, 1998; Lim & Cao, 2006). Last but not least, at the C-terminus end, there is a variable **transactivation domain (TAD)** that helps in the transcription regulation process of target genes, interacting with and recruiting co-activators (like histone acetyltransferases) to the DNA-protein complex. It also contains key phosphorylation residues, such as tyrosines that, once phosphorylated by a

tyrosine kinase (like JAK), facilitate the dimerization and nuclear translocation of STAT proteins. Other serine residues in this domain can modulate the activation of transcription of target genes (Zhang, Li & Watowich, 2016). **Figure 1** presents a comparison between the domains of STAT proteins.

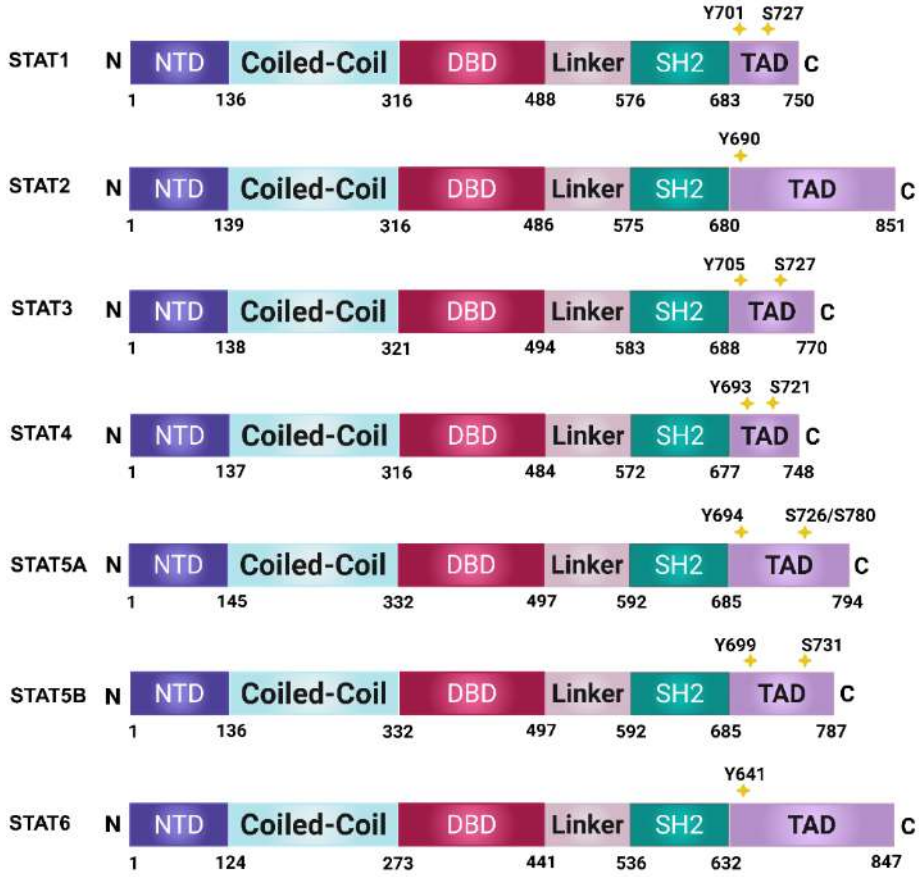

Figure 1: Structural comparison between STAT family members. Created in https://BioRender.com by Puiu Adina-Gabriela (Vasilescu).

To explain the canonical pathway of STAT activation, the generally accepted premise is that STATs exist as inactive monomers in the cytoplasm and require phosphorylation to dimerize (Ivashkiv & Hu, 2004). Specific extracellular signals, like growth factors and cytokines, bind to the corresponding transmembrane receptors. This connection between ligand and receptor determines the tyrosine kinase receptors (such as growth factor receptors) to undergo conformational changes, dimerize and auto-phosphorylate, or non-tyrosine kinase receptors (such as cytokine receptors) to dimerize and to recruit JAKs to the proximity of the cell membrane (Lim & Cao, 2006; Hu et al., 2021). JAKs trans-phosphorylate and trans-activate, further phosphorylating tyrosine residues from the cytoplasmic domain of the receptors. Once phosphorylated, the receptors create docking

sites for STAT proteins (Liang et al., 2024). Upon docking to the receptor, through the recognition of the receptor's phosphotyrosines by the SH2 domain, each STAT molecule is phosphorylated by JAK and dissociates from the receptor (Bild, Turkson & Jove, 2002). Then, phosphorylated STAT proteins homo- or heterodimerize, positioning in an antiparallel orientation through the interaction of their SH2 domains with the phosphotyrosines (Murray, 2007). The dimers translocate to the nucleus *via* nuclear importins and nuclear localization signal (NLS), binding to the promoters of target genes, regulating their transcription (Bild, Turkson & Jove, 2002; Awasthi, Liongue & Ward, 2021). **Figure 2** presents the STAT3 circuit in the cell, as an example of a STAT signaling pathway.

2. STAT3

STAT3 is a key STAT member, being involved in a wide range of cellular processes, such as development, growth and survival. Regulation of STAT3 comprises a plethora of events that take place at different levels and in different cellular compartments, modulating the physiological and pathological STAT3 activity. For example, **Negative regulators** of STAT3 include protein tyrosine phosphatases, the SOCS family and the PIAS family. Several members of the PTP family, like TC-PTP, SHP1, SHP2, PTPRD, or PTPRT, are involved in the dephosphorylation process of STAT3. In triple-negative breast cancer, loss of TC-PTP promotes tumor cell growth by boosting both the activity of Src kinases and STAT3 signaling (Tang, Sui & Liu, 2023). The SOCS protein family works by attaching to JAK kinases or to cytokine receptors that have been activated by JAKs, blocking the phosphorylation and subsequent activation of STAT3 (Tamiya et al., 2011). Also, SOCS are involved in the proteasomal degradation of STAT3 or JAK (Neuwirt et al., 2009). The PIAS family inhibits STAT3 by binding to the formed dimers, thus blocking the DNA interaction and the regulation of downstream genes. PIAS3 stood out as an important negative regulator and high levels of it correlated with reduced cancer cell proliferation and increased apoptosis. Jiang et al. found that defects in SOCS3 and PIAS3 lead to hyperactivation of the JAK/STAT pathway in early-stage breast cancer (Jiang et al., 2020). Another example, **at the post-translational level**, phosphorylation of STAT3 at Tyr 705 is necessary for its activation and is triggered through several signaling types, such as non-receptor tyrosine kinases (like Abl and Src), cytokine receptors and tyrosine kinase receptors (like EGFR or PDGFR) (Michels et al., 2013). STAT3 activation also involves phosphorylation at Ser 727, usually carried out by enzymes like Mitogen-Activated Protein Kinase (MAPK) or Cyclin-dependent kinase 5

(CDK5). Full activation of STAT3 requires both phosphorylation events to occur (Yang et al., 2020).

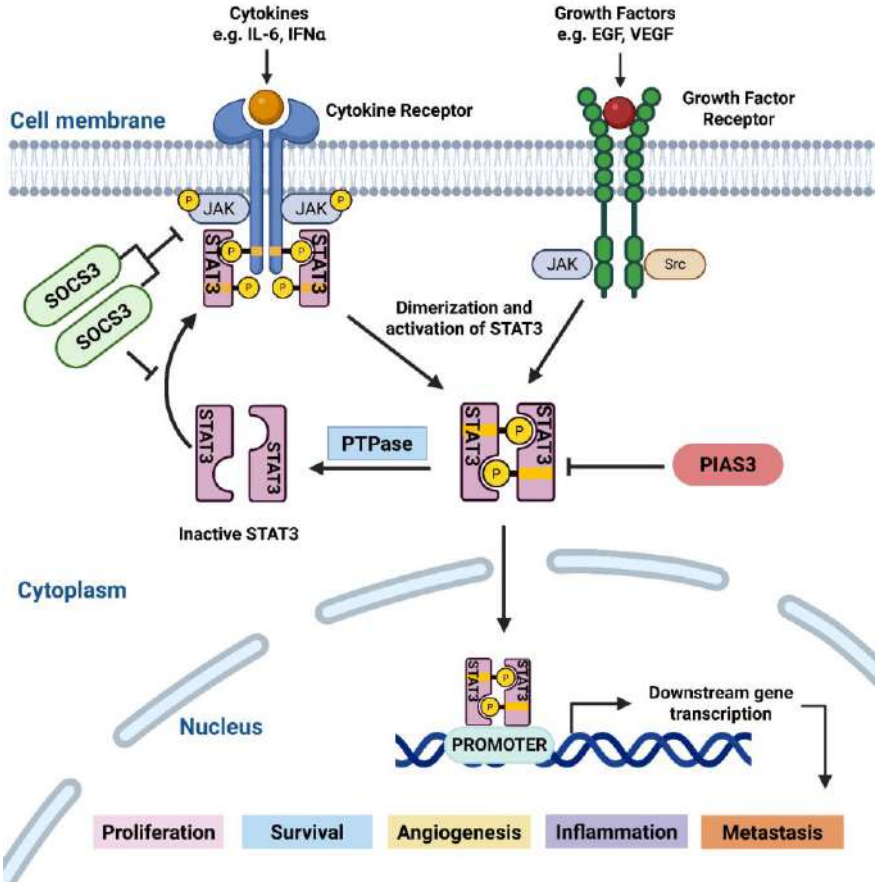

Figure 2: The STAT3 signaling pathway, activated by cytokines or growth factors. The disease-associated biological effects triggered by STAT3 regulation of target genes and some of the negative regulation mechanisms for STAT3 are schematically represented. Created in https://BioRender.com by Puiu Adina-Gabriela (Vasilescu).

STAT3 involvement in Ovarian Cancer (OC)

Activation of STAT3 in OC was correlated with enhanced and persistent proliferation, survival, invasion, blood vessel formation and resistance to chemotherapy by controlling various genes associated with these processes. When activated, STAT3 facilitates the expression of several genes critical for cell proliferation (such as *c-Myc, cyclin D1*, or *Pim-1*) and survival (such as *Bcl-2, Bcl-xL, Mcl-1* and *survivin*). OC cell lines with high levels of phosphorylated STAT3 exhibited increased expression of these downstream effectors, resulting in uncontrolled cell growth and the inhibition of apoptosis (Huang et al., 2000; Wu et al., 2019). STAT3 plays a critical role in the process of angiogenesis. In tumor cells, active STAT3 determines the secretion of high levels of Vascular Endothelial Growth Factor

(VEGF) – a stimulator of STAT3 signaling, which leads to the formation of extra blood vessels. A positive feedback loop involving STAT3 and VEGF supports angiogenesis and drives ovarian cancer progression by enhancing vascularization within the tumor microenvironment (Anglesio et al., 2011). A key enzyme for tumor invasion is matrix metalloproteinase 9 (MMP9), which degrades the extracellular matrix. Phosphorylated STAT3 directly upregulates MMP9, thus contributing to ovarian cancer invasiveness (Cheung, Leung & Wong, 2006; Jia et al., 2017). One step of the metastatic process of OC is the epithelial-to-mesenchymal transition (EMT), characterized by low levels of epithelial markers, like E-cadherin and high levels of mesenchymal markers, like N-cadherin, vimentin and Snail (Davidson, Tropé & Reich, 2012). Hyperactivated STAT3 was correlated with high expression of vimentin in ovarian cancer cells, suggesting that STAT3 is implicated in the EMT process in ovarian cancer (Yue et al., 2012). This relationship between STAT3 and ovarian cancer positions STAT3 as a promising therapeutic target for OC.

Inhibitors of STAT3 signaling

Given the significant role of STAT3 as a biomarker in the development and progression of malignancies, various strategies to inhibit STAT3 signaling have been developed to enhance life expectancy and slow disease progression.

Indirect inhibition refers to those strategies that aim to target and inhibit the upstream molecules in the JAK/STAT3 signaling pathway, like cytokines, cytokine receptors, JAK proteins, or several tyrosine kinases. One example is Siltuximab, an IL-6 inhibitor, which did not show significant effects in advanced-stage tumors, like colorectal, head and neck, or ovarian carcinoma (Angevin et al., 2014). Ruxolitinib or Tofacitinib are JAK inhibitors, but even if they are already FDA-approved, they trigger systemic side effects (Qian, Xue & Shannon, 2022; Verstovsek et al., 2012). Erlotinib, an EGFR inhibitor and Dasatinib, a Src inhibitor, need to be administered together with a chemotherapeutic to present the expected effects, a strategy that increases the toxicity, with systemic damage to the organism (Nagaraj, Washington & Merchant, 2011).

Direct inhibition is exerted by targeting different domains of STAT3 in order to prevent STAT3 activity. Molecules targeting the SH2 domain, which is involved in the interaction of STAT3 with the receptors and also in STAT3 dimerization, have been developed. Peptidomimetics and synthetic small molecules have shown promising effects in cancer (Turkson et al., 2001; Schust et al., 2006). However, they faced limitations like permeability problems, low affinity and off-target effects. Nucleic acid-based strategies, such as antisense

oligonucleotides (ASO), which are designed to bind and degrade the mRNA for STAT3, face limitations like instability and poor specificity despite their potential (Roth, 2005; Zhang et al., 2024).

3. OLIGONUCLEOTIDES AS EFFECTIVE DNA-BINDING DOMAIN INHIBITORS OF STAT3

Once activated and translocated to the nucleus, STAT3 regulates target genes by recognizing and binding through its DNA-binding domain (DBD) specific response elements (like GAS) located in the promoter region of these genes. Several inhibitory molecules, decoy oligonucleotides (ODNs), have been developed to target this domain in order to block the malignancy-driving function of STAT3 and to promote apoptosis and tumor regression.

The first generation of decoys was represented by a linear, double-stranded molecule of 15 bp. This has been extensively used on cancer cell lines for solid tumors and exhibited promising effects. It inhibited proliferation and cell-cycle progression, promoting apoptosis and reducing the expression of STAT3 target genes, like *Cyclin D1, c-myc* and *Bcl-xL* on glioma cells (Gu et al., 2008). It induced apoptosis and reduced cell growth and impaired the interaction of STAT3 with importin, preventing the translocation of STAT3 to the nucleus in colorectal cancer cells (Souissi et al., 2011). After showing encouraging effects on animal models (Zhang et al., 2007; Sen et al., 2009), clinical trials determined that, on systemic administration, the decoy was unstable and rapidly degraded by nucleases (Sen et al., 2012).

Thus, a new class of DNA-based double-stranded molecules, called **DNA minicircles**, has been developed, but this strategy has been insufficiently explored. A method to obtain such circular DNA molecules was proposed by Thibault et al. (2017), inhibiting the NF-κB transcription factor, due to the presence of κB motifs in its sequence, which are recognized by NF-κB. was shown to significantly decrease NF-κB-dependent transcription in HEK293 cells. This study opens up opportunities for designing minicircles as novel decoy nucleic acid tools.

Considering all the information presented so far, namely the importance of the STAT3 protein, as well as its implications in the initiation and progression of ovarian cancer and the promising strategy of using DNA minicircles as potential inhibitors for transcription factors like STAT3, I chose to utilize minicircle DNA directed against STAT3 as a therapeutic agent in ovarian cancer cells as the main focus of this PhD thesis.

III. EXPERIMENTAL PART

1. MATERIALS AND METHODS

The experiments for this thesis were carried out on the SKOV3 ovarian carcinoma cell line, the fifth highest in terms of STAT3 expression level (The Human Protein Atlas, 2025). The oligonucleotides and splints necessary for the production of the anti-STAT3 and mock minicircles (mcDNA) were purchased from GenScript Biotech (Netherlands). The circularization and ligation of the single-stranded molecules were done using the "Double-helical complex splint-assisted enzymatic cyclization of oligonucleotides with T4 DNA ligase" technique (Diegelman & Kool, 2000). The double-stranded molecules were obtained through isolation from the agarose gel of the circular single-stranded molecules, followed by their annealing. The validation of the double-stranded circular conformation was done through enzymatic digestion.

The SKOV3 cells were transfected with the obtained mcDNAs using Lipofectamine 3000 in a DNA: Lipofectamine ratio of 1:1. The IC50 value of the compound was assessed through MTS assay, after treatment with serial concentrations of the anti-STAT3 and mock mcDNA, respectively. SKOV3 cells treated with the anti-STAT3 mcDNA, mock mcDNA, or Lipofectamine-only were next subjected to flow cytometry, quantitative PCR and Western blot to assess the effects of the compound on proliferation, apoptosis and the regulation of STAT3-controlled genes, *MCL1* and *PIM1*. The corresponding statistical tests were applied.

2. RESULTS

The design and the principle of obtaining the minicircles

We employed linear 5′-phosphorylated oligonucleotides (95 nucleotides in length) containing three evenly spaced GAS-like motifs with the sequence **5' TTCCCGTAA 3'**, which serve as recognition sites for the STAT3 DBD, as their sequence has been shown to bind STAT3 with high affinity (Yang et al., 2003). Each complementary strand was individually circularized using the "double-helical complex splint-assisted enzymatic cyclization" method (Diegelman & Kool, 2000), catalyzed by T4 DNA ligase.

This method employs a short single-stranded DNA fragment ("splint") that complements the terminal regions of the oligonucleotide. During the reaction, the oligonucleotide termini are aligned *via* hybridization to the splint, followed by a slow,

controlled ligation step. Maintaining a slow ligation rate increases efficiency and minimizes the formation of undesirable multimers. Following single-strand circularization, products were isolated from agarose gels and annealed with their complementary circles to yield double-stranded anti-STAT3 minicircle DNA (anti-STAT3 mcDNA). A negative control minicircle (mock mcDNA) was generated using scrambled GAS-like motifs that are not recognized by the STAT3 DBD (Vasilescu et al., 2025). **Figure 3** provides an overview of the minicircle production workflow.

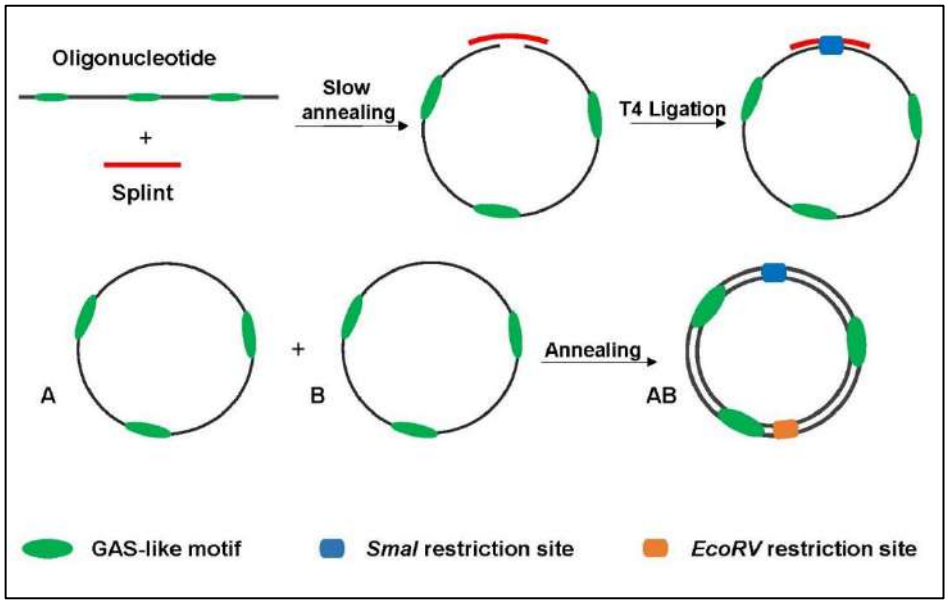

Figure 3: The principle of obtaining the double-stranded minicircles. Schematic representation of the procedure for circularizing oligonucleotides through the splint-assisted enzymatic ligation technique. The mcDNA molecules are created through the annealing of two complementary single-stranded circles. The *SmaI* restriction site serves to confirm successful circularization, whereas *EcoRV* digestion validates the double-stranded nature of the minicircles. This figure is adapted from (Vasilescu et al., 2025).

Production and validation of double-stranded DNA minicircles through enzymatic digestion

To create the anti-STAT3 and mock double-stranded minicircles, we circularized the relevant oligonucleotides using distinct splints, which generated a unique *SmaI* restriction site, as previously described. Purification of the complementary single-stranded circles was followed by their annealing. This hybridization formed the final double-stranded molecules, which included the distinct *EcoRV* restriction site, diametrically opposite to the restriction site for *SmaI*. Consequently, we validated circularization using *SmaI* restriction, whereas the

presence of the *EcoRV* site ensured the full annealing of the two complementary single-stranded circles.

As presented in **Figure 4**, the desired molecule adopts a circular, double-stranded configuration. Following digestion with *SmaI* and *EcoRV* (lane 4), the major product, which is the thicker band, moves significantly lower than the 95-nucleotide linear oligo. The presence of the upper band (or bands) is due to incomplete digestion. *SmaI*-only (lane 5) digestion produces two bands: the upper band indicates the complete double-stranded circular molecule, while the lower band (~100 bp) represents a linear fragment. This pattern is due to partial digestion. *EcoRV*-only (lane 6) digestion generates a unique band near 100 bp, distinct from the final circular product, resembling the lower band seen post-digestion with *SmaI*. We utilized a purified, annealed double-stranded minicircle as a technical negative control, incubating it without restriction enzymes. This control verified the circularity and double-stranded configuration of the synthesized molecules, presenting a unique band, similar to the final circular product.

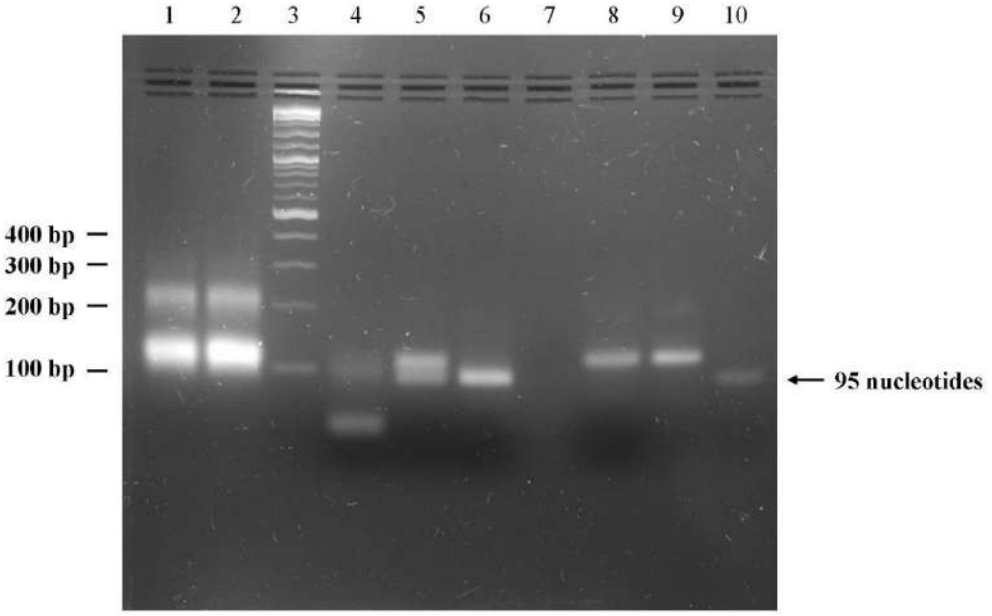

Figure 4: Validation of the double-stranded minicircle against STAT3 in agarose gel. Lane 1: single-stranded minicircle A, resulting from the ligation reaction; Lane 2: single-stranded minicircle B, complementary to minicircle A, resulting from the ligation reaction; Lane 3: Quick-Load® 1 kb Plus DNA Ladder; Lane 4: double-stranded minicircle obtained after purification from gel and annealing, digested with both *SmaI* and *EcoRV* restriction enzymes; Lane 5: double-stranded minicircle obtained after purification and annealing, digested with *SmaI*; Lane 6: double-stranded minicircle obtained after purification and annealing, digested with *EcoRV*; Lane 7: empty; Lane 8: negative control of double-stranded minicircle obtained after purification and annealing, without restriction enzymes; Lane 9: double-stranded minicircle against STAT3, after purification and annealing; Lane 10: linear

oligonucleotide precursor corresponding to single-stranded minicircle A. This figure is adapted from (Vasilescu et al., 2025).

Anti-STAT3 mcDNA specifically interacts with the STAT3 protein

After successfully obtaining and validating the minicircle, we wanted to evaluate the capability of anti-STAT3 mcDNA to interact with the STAT3 protein. We performed an Electrophoretic Mobility Shift Assay (EMSA), utilizing a STAT3 protein obtained in-house. For this assay, we used different molar ratios of DNA: protein.

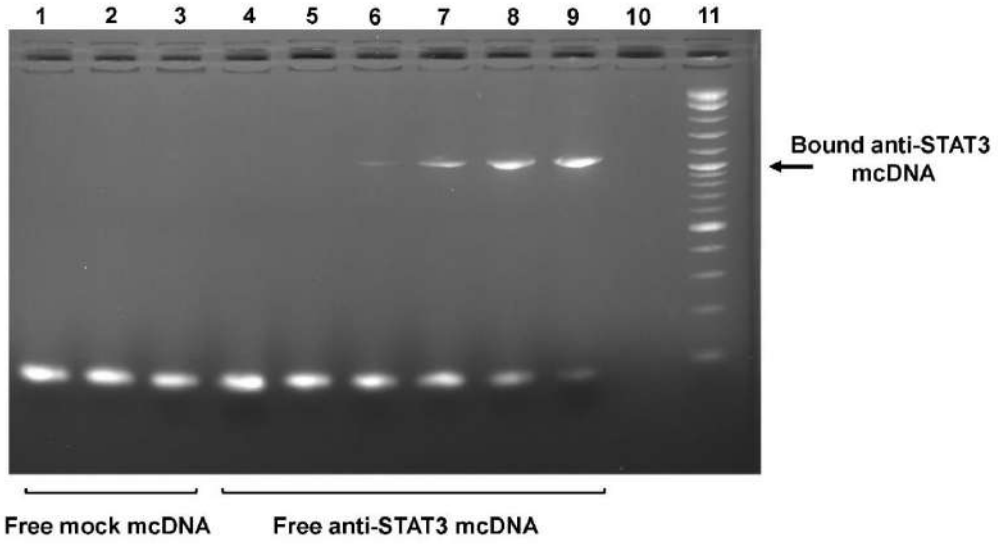

Figure 5: The interaction between the anti-STAT3 mcDNA and STAT3 protein, evidenced through EMSA and displayed on an agarose gel. Different molar ratios of DNA: protein were used for the binding. Lane 1: negative control for mock (mock mcDNA lacking protein); Lanes 2, 3: mock mcDNA: STAT3 in ratios of 1:3 and 1:4; Lane 4: negative control for anti-STAT3 mcDNA (without protein); Lanes 5, 6, 7, 8, 9: anti-STAT3 mcDNA: STAT3 in ratios of 1:0.75, 1:1.5, 1:2, 1:3 and 1:4; Lane 10: empty lane; Lane 11: Quick-Load® 1 kb Plus DNA Ladder. This figure is adapted from (Vasilescu et al., 2025).

The agarose gel from **Figure 5** presents two types of bands: (i) bands that migrate around 100 bp, corresponding to the free form of minicircle, the one that did not interact with the protein, or whose interaction was extremely weak, such as the DNA molecule was not delayed; (ii) bands with markedly reduced mobility (well above the 100 bp region), consistent with high-molecular-weight STAT3–mcDNA complexes; the pronounced shift may reflect multimeric binding of STAT3 dimers or partial aggregation of the protein–DNA complex. The strength of the interaction and mass of the interacting protein dictate the degree of delay of the DNA molecule during migration. At the molar ratio of 1:0.75 (lane 5), there seems to be no interaction between anti-STAT3 mcDNA and STAT3 protein, with only the

free form being present. The same is true for the negative control (lane 4, without protein). In the molar ratio range of 1:1.5 to 1:4, an increase in the bound form and a decrease in the free form of anti-STAT3 mcDNA can be observed. From these results, it seems that for a successful interaction, the protein must be in molar excess over the DNA. The mock mcDNA incubated with the protein in molar ratios of 1:3 and 1:4 displays the same migration pattern as the mock negative control (without protein), with no shift in migration for the DNA molecule. This suggests that mock mcDNA, due to the scrambled GAS-like motifs it contains, does not interact with the STAT3 protein. These findings indicate that anti-STAT3 mcDNA specifically interacts with the STAT3 protein, due to its GAS-like motifs.

Anti-STAT3 mcDNA treatment lowers the viability of ovarian cancer SKOV3 cells

SKOV3 cells were transfected with either anti-STAT3 mcDNA or mock mcDNA (negative control for specificity) in the serial concentrations: 0 nM, 1.56 nM, 3.12 nM, 6.25 nM, 12.5 nM, 25 nM, 50 nM and 100 nM. Technical triplicates of each condition were performed. The technical negative controls for this technique were represented by the untreated cells and Lipofectamine 3000-only-treated cells in equivalent DNA concentrations of 25 nM, 50 nM and 100 nM. The technical positive control was represented by a 15-minute incubation with Triton X-100 0.02%, before adding the MTS reagent.

After performing the MTS assay, we obtained an IC_{50} value of 13.48 nM for anti-STAT3 mcDNA. **Figure 6A** illustrates the fact that the cell viability was reduced in a dose-dependent fashion relative to the cells treated only with Lipofectamine. In contrast, the treatment with mock mcDNA did not register any notable effect on cell viability, regardless of concentration. We wanted to evaluate the toxic effect of Lipofectamine at the highest concentrations applied (25 nM, 50 nM and 100 nM) and to determine whether the observed effect is due exclusively to treatment with the DNA compound, or the effect of Lipofectamine also intervenes. To this end, we compared the untreated cells with the Lipofectamine-only treated cells, the anti-STAT3 mcDNA treated cells at 25 nM, 50 nM and 100 nM and the Triton X-100 treated cells (**Figure 6B**). For instance, we observed a statistically significant difference in the viability of the cells between Lipofectamine-only treatment and anti-STAT3 mcDNA treatment in the case of all three concentrations. In conclusion, even if there is Lipofectamine toxicity, it can be considered that most of the observed effects are due to the minicircle treatment. Further, we observed a statistically significant effect on Lipofectamine-only treated cells at equivalent DNA concentrations of

50 nM and 100 nM, when compared to untreated cells. Also, when it comes to Lipofectamine-only treated cells at an equivalent DNA concentration of 25 nM, no significant toxic effect was observed, compared to untreated cells. Thus, the decrease in cell viability registered at the IC_{50} was solely a result of the anti-STAT3 mcDNA treatment.

These findings, along with the minimal impact of mock mcDNA treatment, validate the targeted inhibitory action of anti-STAT3 mcDNA (Vasilescu et al., 2025).

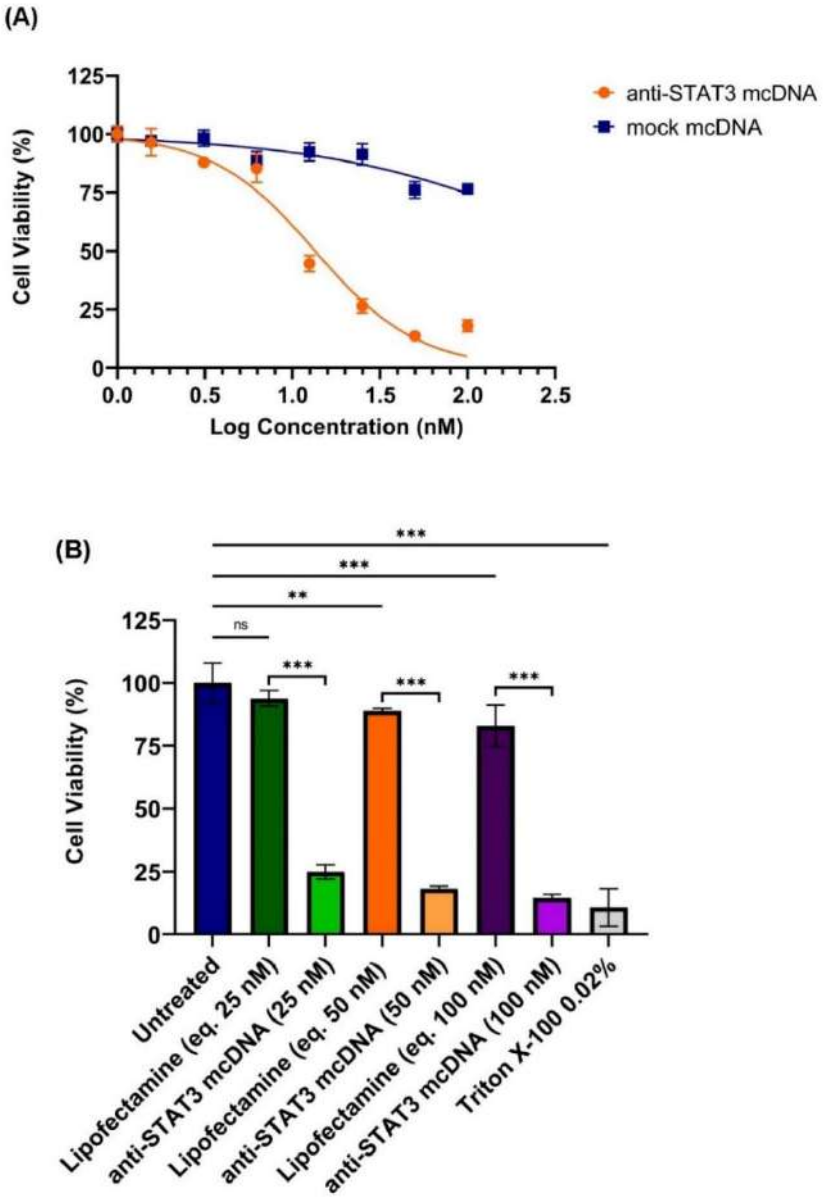

Figure 6: The inhibition impact of anti-STAT3 mcDNA on SKOV3 ovarian cancer cells, evaluated using the MTS assay. **(A)** The effects of anti-STAT3 mcDNA and mock mcDNA treatments of SKOV3 cells, illustrated through inhibitory dose-response curves. Data points indicate the average percentage of cell viability normalized to Lipofectamine-only samples at the tested treatment concentrations: 0 nM, 1.56 nM, 3.12 nM, 6.25 nM, 12.5 nM, 25 nM, 50 nM, and 100 nM. **(B)** The evaluation of the toxic effect of Lipofectamine 3000 administered alone on SKOV3 cells at equivalent DNA concentrations (25 nM, 50 nM and

100 nM), compared to anti-STAT3 mcDNA-treated, untreated and Triton X-100-treated conditions. Statistical significance was assessed using one-way ANOVA. ns – not significant ($p \geq 0.05$); * $p<0.05$; ** $p<0.01$; *** $p<0.001$. Error bars represent ± SD. Results are presented from one representative experiment out of three conducted ($n=3$). This figure is adapted from (Vasilescu et al., 2025).

Anti-STAT3 mcDNA treatment induces apoptosis and necrosis in SKOV3 cells

Seeing as the MTS results indicate that the anti-STAT3 mcDNA treatment decreased the viability of SKOV3 cells, we examined the effects of this compound in terms of apoptosis and necrosis of ovarian cancer cells.

We transfected the cells with three different concentrations of anti-STAT3 minicircle or mock minicircle: 5 nM, 10 nM and 20 nM, to observe whether a dose-dependency exists. The flow cytometry protocol was employed by staining with Annexin V-FITC and PI (markers for apoptosis and necrosis, respectively). As shown in **Figure 7A**, the anti-STAT3 mcDNA treatment led to an increase in the percentage of apoptotic (lower right quadrant, stained Annexin V^+, PI^-) and necrotic (upper right quadrant, stained Annexin V^+, PI^+) cells, across all three applied concentrations, while mock mcDNA treatment (which is the specificity negative control, according to the previous results) showed almost no effect on cell apoptosis or necrosis. Also, the effect of mock mcDNA is similar to the effect of Lipofectamine-only (technical negative control, equivalent DNA concentration of 20 nM) treatment and similar to the percentages in necrosis and apoptosis observed in untreated cells (technical negative control). Even at 5 nM compound (lower than half the IC_{50}), there was a pronounced effect, resulting in 76.97% viable cells, 13.61% apoptotic and 9.18% necrotic. In the case of the anti-STAT3 mcDNA treatment, there is a slight increase in apoptosis and necrosis and a decrease in viable cells between the 5 nM and 10 nM treatments. However, we did not observe the same trend of increasing apoptosis and necrosis between 10 nM and 20 nM, indicating that the pro-apoptotic effect plateaus between 10 nM and 20 nM. **Figure 7B** shows the controls for this analysis: untreated cells, Lipofectamine-only treated cells, CisPlatin (technical positive control for apoptosis) and Triton X-100 (technical positive control for necrosis). In conclusion, inhibition of STAT3 activity through the treatment with the minicircle compound promotes apoptosis and necrosis in SKOV3 ovarian cancer cells

dose-dependently in the range of 0 nM to 10 nM, plateauing at higher concentrations.

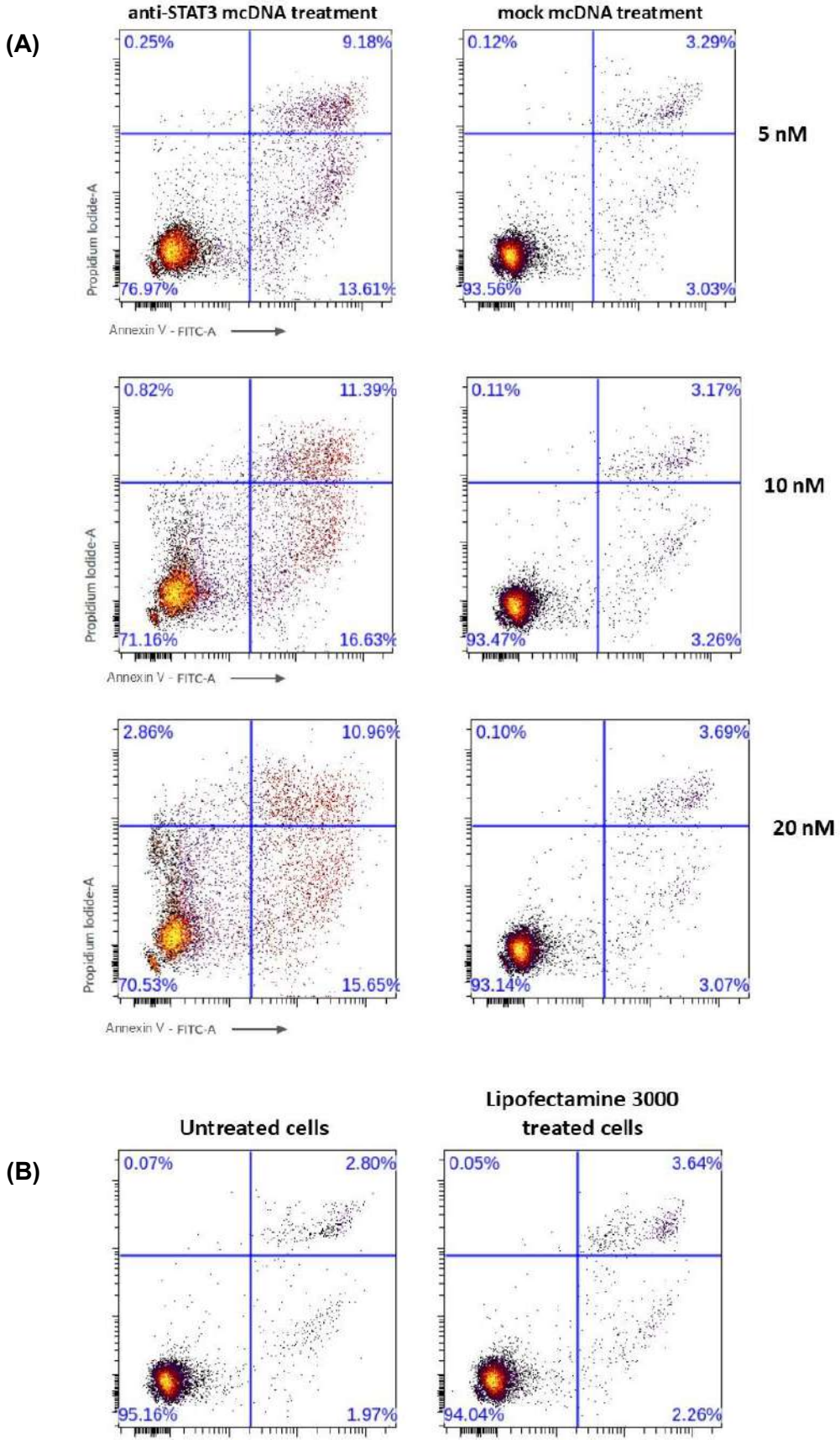

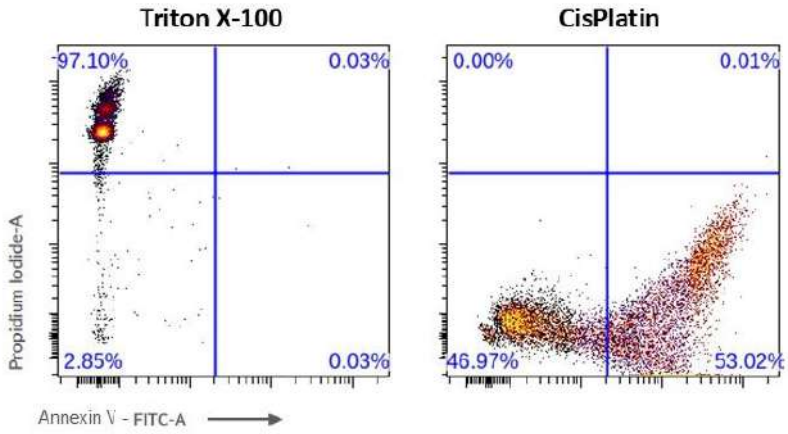

Figure 7: Impact of anti-STAT3 mcDNA treatment on apoptosis and necrosis in SKOV3 ovarian cancer cells. **(A)** Proportion of apoptotic and necrotic cells after treatment with anti-STAT3 mcDNA in comparison to the mock control in different concentrations (5 nM, 10 nM and 20 nM, respectively). The lower right quadrant represents apoptotic cells (Annexin V^+, PI^-), while the upper right quadrant represents necrotic cells (Annexin V^+, PI^+). **(B)** The negative (Untreated and Lipofectamine 3000-treated samples) and positive (Triton X-100 and CisPlatin-treated samples) controls for apoptosis and necrosis. The data present the findings from one representative experiment. This figure is adapted from (Vasilescu et al., 2025).

Anti-STAT3 mcDNA reduces the proliferation of SKOV3 ovarian cancer cells

In order to identify the further molecular effects that our minicircle triggers through STAT3 inhibition on ovarian cancer cells, we explored the proliferation process. We used SKOV3 cell lysates to evaluate the protein levels of Ki-67, cleaved caspase 3, STAT3, STAT3 phosphorylated at Tyr705 and GAPDH, using the Western blot technique. The treatment concentration was 10 nM. As shown in **Figure 8A**, in the case of treatment of SKOV3 cells with anti-STAT3 mcDNA, the expression levels of Ki-67 (proliferation marker), normalized to GAPDH (as loading control), were found to be more than two-fold reduced compared to those of Lipofectamine-only (technical negative control), or mock mcDNA-treated cells (experimental negative control). This difference is statistically significant. However, Ki-67 expression levels between Lipofectamine and mock-treated cells are similar (**Figure 8C**). Moreover, cleaved caspase 3 (**Figure 8A**), a marker of apoptosis, was detected only in anti-STAT3 mcDNA-treated cells. Due to its low expression levels, it was evaluated qualitatively rather than quantitatively. These findings support the flow cytometry conclusions, which indicate that our compound is capable of inducing apoptosis of ovarian cancer cells. Also, treatment with this inhibitory molecule impairs ovarian cancer cell proliferation.

Although a slight reduction in STAT3 expression was observed in SKOV3 treated with anti-STAT3 mcDNA, compared to the cells treated with Lipofectamine or mock mcDNA, this reduction was not statistically significant (**Figure 8C**). In the case of phosphorylated STAT3, there is a considerable difference (**Figures 8B and C**). After the treatment with anti-STAT3 mcDNA, the expression levels of phospho-STAT3 (Tyr705) were significantly lower compared to Lipofectamine-only or mock mcDNA-treated cells. Between the Lipofectamine and mock treatments, the levels of phospho-STAT3 are comparable and suggest that the active STAT3 protein is present. In contrast, the low levels of phospho-STAT3 observed in cells treated with anti-STAT3 minicircle show that there is less active STAT3 or that STAT3 is no longer activated, suggesting a disrupted signaling in the JAK/STAT3 pathway.

In conclusion, the protein expression analysis strengthens the MTS and flow cytometry results, showing that the treatment of SKOV3 cells with anti-STAT3 mcDNA induces high levels of apoptosis, while also inhibiting STAT3 signaling and leading to reduced cell proliferation.

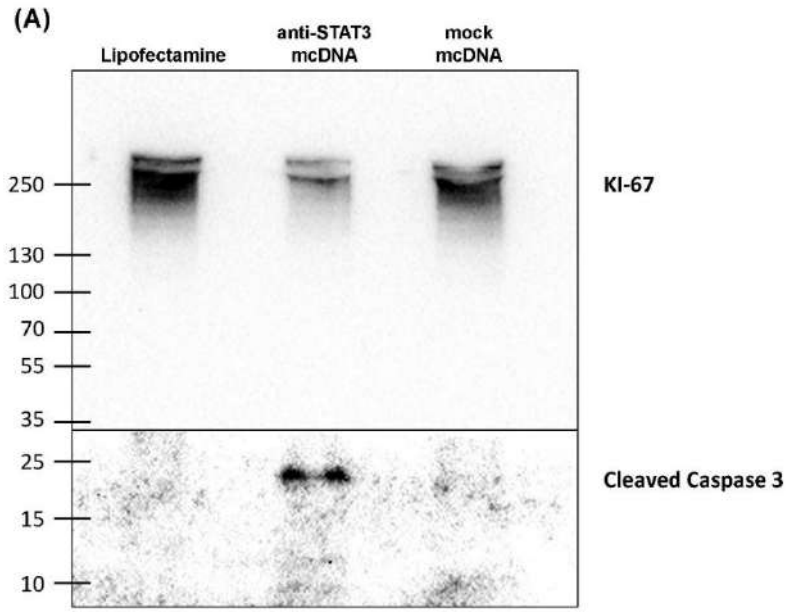

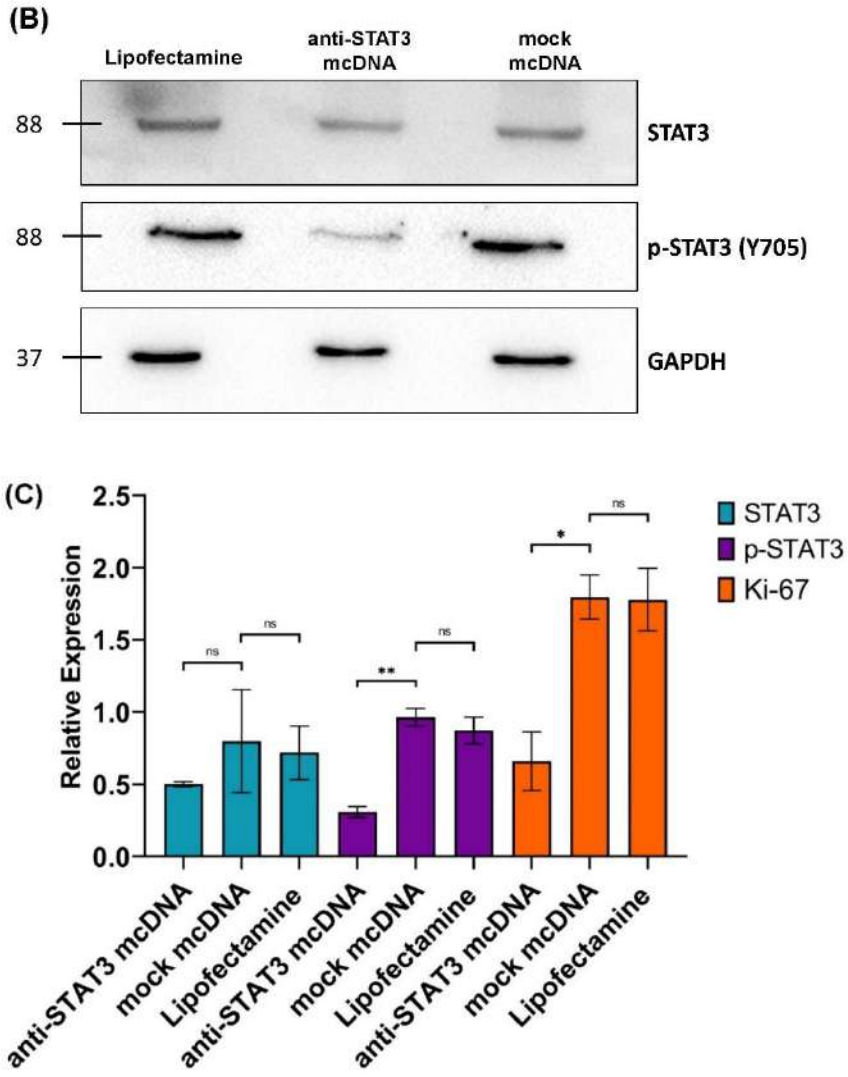

Figure 8: Analysis of SKOV3 cell lysates using the Western blot technique. **(A)** In SKOV3 cells, the expression levels of Ki-67 (>250 kDa) and cleaved caspase 3 (~20 kDa) were analyzed following the treatment with Lipofectamine 3000 alone (equivalent DNA concentration), anti-STAT3 mcDNA and mock mcDNA at a concentration of 10 nM. Cleaved caspase 3 was visualized using SuperSignal™. The ladder used to visualize and validate these proteins is schematically indicated on the left (PageRuler™ Plus Prestained Protein Ladder, 10 to 250 kDa); **(B)** The protein expression levels of STAT3, p-STAT3 (Y705) and GAPDH, determined in SKOV3 cells after the above-mentioned treatment conditions. The corresponding molecular weights are indicated on the left; **(C)** Quantification of STAT3, p-STAT3, and Ki-67 expression levels, normalized to GAPDH as loading control, throughout treatments. Cleaved caspase-3 appears as either present or absent because of its low expression levels. Statistical significance was assessed using a one-tailed unpaired *t*-test. ns – not significant ($p \geq 0.05$); * $p < 0.05$; ** $p < 0.01$. Error bars indicate ± SEM. The figure shows one representative experiment ($n=3$). This figure is adapted from (Vasilescu et al., 2025).

Anti-STAT3 minicircle decreases pro-survival and anti-apoptotic gene expression

Given the regulatory function of STAT3 for numerous genes involved in the growth, proliferation and survival of cancer cells, we wanted to further investigate whether the expression of certain STAT3 downstream genes is affected, once the activity of STAT3 is inhibited by anti-STAT3 mcDNA. The motivation for this is that the inhibition of STAT3 downstream genes could be a reason for the phenotypes detected in MTS and flow cytometry in anti-STAT3 mcDNA-treated cells. For this purpose, two STAT3-regulated genes, *MCL1* and *PIM1*, with established roles in apoptosis inhibition and cell survival (Shirogane et al., 1999; Kanda et al., 2004), were selected for expression analysis through RT-qPCR. We treated SKOV3 cells with 10 nM of the anti-STAT3 minicircle or the mock minicircle, respectively. For these experiments, we used technical duplicates. As illustrated in **Figure 9**, both genes exhibited significant downregulation in cells treated with anti-STAT3 mcDNA, in comparison to mock mcDNA (experimental negative control) treatment. Specifically, *MCL1* levels decreased by around 50%, whereas *PIM1* levels were diminished by approximately 75%, as determined through comparative quantitation analysis.

These molecular findings complement the previously observed reduction in ovarian cancer cell viability and increased apoptosis upon anti-STAT3 mcDNA treatment, by providing a mechanistic link between STAT3 inhibition and impairment of cell function.

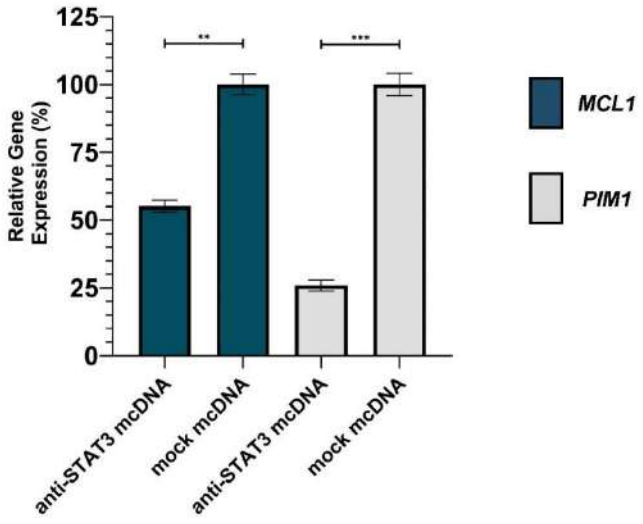

Figure 9: Quantification of the Relative Gene Expression *via* RT-qPCR for the *MCL1* and *PIM1* genes. The cells were subjected to the anti-STAT3 or mock mcDNA treatment at 10 nM concentration and the data were normalized to *GAPDH* gene expression levels. A one-tailed unpaired *t*-test was employed to assess statistical significance. ** $p<0.01$; *** $p<0.001$. Error bars indicate ± SD. Data presents the findings from one representative

experiment among three conducted (*n*=3). This figure is adapted from (Vasilescu et al., 2025).

After the qPCR results shed light on the gene expression levels, we wanted to further investigate what happens with the corresponding protein levels when the cells are treated with our minicircle. Thus, we investigated the SKOV3 cell lysates through Western blot, after treatment with 10 nM concentration. As **Figure 10A** shows, after the treatment with anti-STAT3 mcDNA, the expression levels of Mcl-1 protein were significantly reduced by over two-fold (**Figure 10C**) compared to mock mcDNA treatment (experimental negative control), aligning with the results obtained from the mRNA analysis. Mock mcDNA-treated cells showed Mcl-1 levels similar to those treated solely with Lipofectamine (technical negative control). Regarding the expression level of Pim-1, given the low quantity of the protein, quantification was not possible. In **Figure 10B**, the black arrows mark the hardly detectable bands corresponding to the Pim-1 protein. There was no band observed in the anti-STAT3 mcDNA-treated condition.

The Real-Time qRT-PCR and Western blot data suggest that anti-STAT3 mcDNA is capable of down-regulating STAT3-targeted anti-apoptotic and pro-survival genes, leading to reduced survival and growth of SKOV3 ovarian cancer cells (Vasilescu et al., 2025). Together, these results provide strong evidence that anti-STAT3 mcDNA not only reduces STAT3 activation and function, but also diminishes the expression of key downstream effectors involved in tumor cell survival and proliferation. The observed downregulation of *MCL1* and *PIM1* further supports the therapeutic potential of this synthetic construct as a targeted inhibitor of the JAK/STAT3 signaling axis in ovarian cancer cells.

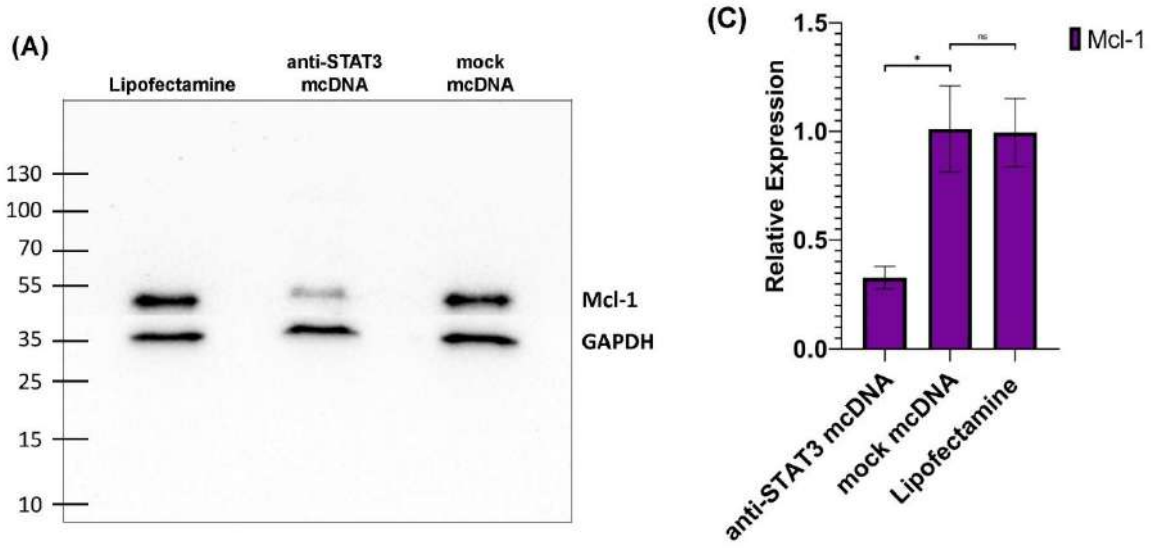

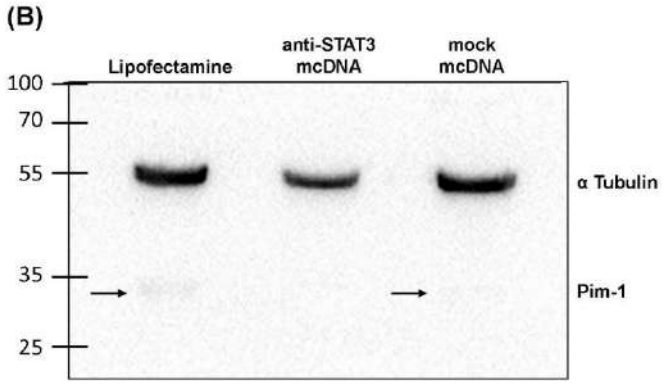

Figure 10: Analysis of SKOV3 cell lysates, using the Western blot approach. **(A)** Expression levels of Mcl-1 and GAPDH in the SKOV3 cells treated with Lipofectamine 3000 only (equivalent DNA concentration), anti-STAT3 mcDNA and mock mcDNA at 10 nM concentration. The ladder used to visualize and validate these proteins is schematically indicated on the left (PageRuler™ Plus Prestained Protein Ladder, 10 to 250 kDa); **(B)** Protein expression levels of Pim-1 and α Tubulin in SKOV3 cells in the same treatment conditions. The black arrows indicate the bands of Pim-1 protein, which was detected only as either present or absent because of its very low abundance. The protein was visualized using SuperSignal™. Part of the ladder is indicated on the left. **(C)** Quantification of Mcl-1 expression levels normalized to GAPDH throughout the treatment conditions. Statistical significance was evaluated with a one-tailed unpaired *t*-test. ns – not significant ($p \geq 0.05$); * $p < 0.05$. Error bars indicate ± SEM. Data from a representative experiment ($n=3$). This figure is adapted from (Vasilescu et al., 2025).

Limitations of the study

This study represents a proof-of-concept and does not encompass the full scope of pre-clinical evaluation for the proposed compound. One major limitation is the exclusive use of a single ovarian cancer cell line (SKOV3), which restricts the generalizability of the results across diverse genetic backgrounds. Additionally, the study lacks in vivo validation, which is essential for evaluating the compound's pharmacokinetics, biodistribution, and therapeutic efficacy in a more physiologically relevant context. Although the anti-STAT3 minicircle is structurally designed to be highly stable and nuclease-resistant, no *in vivo* delivery strategy has been tested thus far. The gel-based purification method used here, while sufficient for *in vitro* experiments, is not scalable for the large quantities required for animal studies. Therefore, the development of an alternative purification technique is necessary for future pre-clinical testing. Furthermore, while the minicircle clearly impairs STAT3 activity *in vitro*, the exact mechanism of action remains to be elucidated. It is not yet clear whether the observed effects result from competitive binding to DNA response elements, sequestration of STAT3 in the cytoplasm, inhibition of dimerization, or disruption of

upstream signaling. Future mechanistic studies are needed to clarify these possibilities. These aspects must be addressed in subsequent animal models to determine the clinical relevance and safety of the anti-STAT3 minicircle.

Perspectives

To address these limitations, in future studies, we intend to evaluate our compound's efficacy on multiple ovarian carcinoma cell lines with varying genetic profiles and to test its stability when injected *in vivo*, determining its potency in xenograft models. To overcome scalability limitations, annealing could be performed immediately after the ligation step, and the final product purified via HPLC, allowing higher-yield production for animal studies. Additionally, we plan to employ an *in vivo* delivery strategy, such as the use of solid lipid nanoparticles (SLNs) (Akanda, Mithu & Douroumis, 2023) to facilitate targeted transport of the anti-STAT3 mcDNA. These carriers can be functionalized with antibodies or affibodies recognizing ovarian cancer-specific biomarkers, enhancing cellular uptake and specificity. Such a Trojan horse approach could allow for minimized off-target effects and immune tolerance to the construct, supporting the development of a personalized, targeted decoy therapy based on DNA minicircles.

IV. CONCLUSIONS

- Ovarian cancer is commonly known as „the silent killer", given that its initial symptoms are unclear and can be easily misinterpreted, resulting in late diagnosis and treatment. Thus, targeted personalized therapy has the potential to improve long-term survival.
- We created the design of an anti-STAT3 and a mock minicircle and we optimized the protocol for their production.
- We successfully obtained and validated the anti-STAT3 mcDNA, along with its mock counterpart, using enzymatic cyclization and restriction digestion, confirming its circular, double-stranded conformation, which is expected to confer resistance to nucleases and enhance stability compared to linear ODN-decoys.
- The specificity of the anti-STAT3 minicircle was confirmed by demonstrating its interaction with the STAT3 protein, in contrast to mock mcDNA.

- ❖ Functional assays demonstrated that anti-STAT3 mcDNA significantly reduced SKOV3 cell viability in a dose-dependent manner, with an IC_{50} within the low nanomolar range, indicating high potency. Importantly, the mock mcDNA did not affect cell viability, confirming the specificity of the GAS-like motifs for STAT3 inhibition.
- ❖ Anti-STAT3 mcDNA effectively shifts the balance toward apoptosis and necrosis, while reducing proliferative capacity in ovarian cancer cells.
- ❖ Mechanistically, treatment with anti-STAT3 mcDNA resulted in a significant downregulation of STAT3-regulated anti-apoptotic and pro-survival genes, *MCL1* and *PIM1*, at the mRNA and protein levels.
- ❖ While our study demonstrates the efficacy of anti-STAT3 mcDNA *in vitro*, it forms the basis for further evaluating its stability, biodistribution and therapeutic potential *in vivo*.

ACKNOWLEDGEMENTS

First of all, I would like to express my enormous gratitude to my PhD coordinator, Prof. Dr. Ștefan-Eugen Szedlacsek, who gave me the opportunity to carry out my work as a PhD student within the Enzymology Department from the Institute of Biochemistry of the Romanian Academy. He guided me through the scientific problems, helping in the conceptualization of the experimental ideas, showed patience and understanding. I would also like to thank my colleagues from the Enzymology Department because together, we formed a family: Andrei-Mihai Vasilescu, Andra-Elena Coşoreanu-Șulea, Cătălin-Constantin Bica and Otilia-Cristina Donţu

I express my gratitude to Prof. Dr. Eyal Arbely from the Department of Chemistry, Ben-Gurion University of the Negev, Israel, who generously gifted us the STAT3 plasmid. I also thank the Department of Viral Glycoproteins, from the Institute of Biochemistry of the Romanian Academy, for providing the anti-α Tubulin antibody and the Lipofectamine 3000.

List of publications relevant to the PhD training

1. **Vasilescu, A.-G.,** Vasilescu, A.-M., Sima, L. E., Baran, N. & Szedlacsek, Ș.-E. 2025. Breaking the cancer code: a novel DNA minicircle to disable STAT3 in ovarian cancer cells SKOV3. Front. Pharmacol. 16:1673427. DOI: 10.3389/fphar.2025.1673427.
2. Váradi, B., Brezovcsik, K., Garda, Z., Madarasi, E., Szedlacsek, H., Badea, R.-A., Vasilescu, A.-M., **Puiu, A.-G.,** Ionescu, A. E., Sima, L.-E., Munteanu, C. V. A., Călăraș, S., Vágner, A., Szikra, D., Toàn, N. M., Nagy, T., Szűcs, Z., Szedlacsek, S., Nagy, G. & Tirscó, G. 2023. Synthesis and characterization of a novel [52Mn]Mn-labelled affibody based radiotracer for HER2+ targeting. Inorg. Chem. Front. 10. 4734– 4745. DOI: 10.1039/D3QI00356F.
3. Vasilescu, A.-M., **Vasilescu, A.-G.,** Sima, L. E., Munteanu, C. V. A., Baran, N. & Szedlacsek, Ș.-E. 2025. A novel cytotoxic anti-B7-H3 affibody with therapeutic potential in acute myeloid leukemia. Front. Pharmacol. 16:1684226. DOI: 10.3389/fphar.2025.1684226.

Posters:

1. **Puiu, A.,** Vasilescu, A. & Szedlacsek, S. 2025. Development of a novel small circular DNA decoy inhibitor targeting STAT3 for cancer therapy. *FEBS Open Bio*. 15:P-32-102. DOI: 10.1002/2211-5463.70071. *The 49th FEBS Congress 2025*. Istanbul.
2. Vasilescu, A., **Puiu, A.** & Szedlacsek, S. 2025. A novel cytotoxic fusion protein targeting B7-H3 for acute myeloid leukemia therapy. *FEBS Open Bio*. 15:P-32-103. DOI: 10.1002/2211-5463.70071. *The 49th FEBS Congress 2025*. Istanbul.
3. Váradi B., Z. Garda Z., Madarasi E., Brezovcsik K., Vágner A., Nagy T., Garai I. M., **Puiu A. G.**, Vasilescu A. M., Szűcs Z., Szedlacsek S. E., Nagy G. & Tirfél Gy. 2022. Labeling of anti-HER2-affibodies with 52Mn via pyclen-based bifunctional ligands: from ligand design to in vivo PET / MR experiments, 35th Annual Congress of the European Association of Nuclear Medicine 2022. Barcelona.

REFERENCES

1. Akanda, M., Mithu, M.S.H. & Douroumis, D. 2023. Solid lipid nanoparticles: An effective lipid-based technology for cancer treatment. *Journal of Drug Delivery Science and Technology*. 86:104709. DOI: 10.1016/J.JDDST.2023.104709.
2. Angevin, E., Tabernero, J., Elez, E., Cohen, S.J., Bahleda, R., Van Laethem, J.L., Ottensmeier, C., Lopez-Martin, J.A., et al. 2014. A phase I/II, multiple-dose, dose-escalation study of siltuximab, an anti-interleukin-6 monoclonal antibody, in patients with advanced solid tumors. *Clinical cancer research : an official journal of the American Association for Cancer Research*. 20(8):2192–2204. DOI: 10.1158/1078-0432.CCR-13-2200.
3. Anglesio, M.S., George, J., Kulbe, H., Friedlander, M., Rischin, D., Lemech, C., Power, J., Coward, J., et al. 2011. IL6-STAT3-HIF signaling and therapeutic response to the angiogenesis inhibitor sunitinib in ovarian clear cell cancer. *Clinical cancer research : an official journal of the American Association for Cancer Research*. 17(8):2538–2548. DOI: 10.1158/1078-0432.CCR-10-3314.
4. Awasthi, N., Liongue, C. & Ward, A.C. 2021. STAT proteins: a kaleidoscope of canonical and non-canonical functions in immunity and cancer. *Journal of Hematology & Oncology*. 14(1):198. DOI: 10.1186/S13045-021-01214-Y.
5. Baran, P., Hansen, S., Waetzig, G.H., Akbarzadeh, M., Lamertz, L., Huber, H.J., Reza Ahmadian, M., Moll, J.M., et al. 2018. The balance of interleukin (IL)-6, IL-6soluble IL-6 receptor (sIL-6R), and IL-6sIL-6Rsgp130 complexes allows simultaneous classic and trans-signaling. *Journal of Biological Chemistry*. 293(18):6762–6775. DOI: 10.1074/JBC.RA117.001163.
6. Becker, S., Groner, B. & Müller, C.W. 1998. Three-dimensional structure of the Stat3β homodimer bound to DNA. *Nature*. 394(6689):145–151. DOI: 10.1038/28101.
7. Bild, A.H., Turkson, J. & Jove, R. 2002. Cytoplasmic transport of Stat3 by receptor-mediated endocytosis. *The EMBO Journal*. 21(13):3255. DOI: 10.1093/EMBOJ/CDF351.
8. Calò, V., Migliavacca, M., Bazan, V., Macaluso, M., Buscemi, M., Gebbia, N. & Russo, A. 2003. STAT proteins: from normal control of cellular events to tumorigenesis. *Journal of cellular physiology*. 197(2):157–168. DOI: 10.1002/JCP.10364.

9. Cheung, L.W.T., Leung, P.C.K. & Wong, A.S.T. 2006. Gonadotropin-releasing hormone promotes ovarian cancer cell invasiveness through c-Jun NH2-terminal kinase-mediated activation of matrix metalloproteinase (MMP)-2 and MMP-9. *Cancer research*. 66(22):10902–10910. DOI: 10.1158/0008-5472.CAN-06-2217.
10. Davidson, B., Tropé, C.G. & Reich, R. 2012. Epithelial–Mesenchymal Transition in Ovarian Carcinoma. *Frontiers in Oncology*. 2(APR):33. DOI: 10.3389/FONC.2012.00033.
11. Diegelman, A.M. & Kool, E.T. (in press). Chemical and Enzymatic Methods for Preparing Circular Single-Stranded DNAs . *Current Protocols in Nucleic Acid Chemistry*. 00(1):5.2.1-5.2.27. DOI: 10.1002/0471142700.NC0502S00.
12. Goumas, F.A., Holmer, R., Egberts, J.H., Gontarewicz, A., Heneweer, C., Geisen, U., Hauser, C., Mende, M.M., et al. 2015. Inhibition of IL-6 signaling significantly reduces primary tumor growth and recurrencies in orthotopic xenograft models of pancreatic cancer. *International journal of cancer*. 137(5):1035–1046. DOI: 10.1002/IJC.29445.
13. Gu, J., Li, G., Sun, T., Su, Y., Zhang, X., Shen, J., Tian, Z. & Zhang, J. 2008. Blockage of the STAT3 signaling pathway with a decoy oligonucleotide suppresses growth of human malignant glioma cells. *Journal of neuro-oncology*. 89(1):9–17. DOI: 10.1007/S11060-008-9590-9.
14. Hendry, L. & John, S. 2004. Regulation of STAT signalling by proteolytic processing. *European Journal of Biochemistry*. 271(23–24):4613–4620. DOI: 10.1111/J.1432-1033.2004.04424.X.
15. Horvath, C.M., Wen, Z. & Darnell, J.E. 1995. A STAT protein domain that determines DNA sequence recognition suggests a novel DNA-binding domain. *Genes & development*. 9(8):984–994. DOI: 10.1101/GAD.9.8.984.
16. Hu, X., li, J., Fu, M., Zhao, X. & Wang, W. 2021. The JAK/STAT signaling pathway: from bench to clinic. *Signal Transduction and Targeted Therapy*. 6(1):1–33. DOI: 10.1038/S41392-021-00791-1.
17. Huang, M., Page, C., Reynolds, R.K. & Lin, J. 2000. Constitutive activation of Stat 3 oncogene product in human ovarian carcinoma cells. *Gynecologic Oncology*. 79(1):67–73. DOI: 10.1006/gyno.2000.5931.
18. Ivashkiv, L.B. & Donlin, L.T. 2014. Regulation of type i interferon responses. *Nature Reviews Immunology*. 14(1):36–49. DOI: 10.1038/NRI3581.

19. Ivashkiv, L.B. & Hu, X. 2004. Signaling by STATs. *Arthritis Research & Therapy*. 6(4):159. DOI: 10.1186/AR1197.
20. Jia, Z.H., Jia, Y., Guo, F.J., Chen, J., Zhang, X.W. & Cui, M.H. 2017. Phosphorylation of STAT3 at Tyr705 regulates MMP-9 production in epithelial ovarian cancer. *PloS one*. 12(8). DOI: 10.1371/JOURNAL.PONE.0183622.
21. Jiang, M., Zhang, W., Zhang, R., Liu, P., Ye, Y., Yu, W., Guo, X. & Yu, J. 2020. Cancer exosome-derived miR-9 and miR-181a promote the development of early-stage MDSCs via interfering with SOCS3 and PIAS3 respectively in breast cancer. *Oncogene*. 39(24):4681–4694. DOI: 10.1038/S41388-020-1322-4.
22. Kanda, N., Seno, H., Konda, Y., Marusawa, H., Kanai, M., Nakajima, T., Kawashima, T., Nanakin, A., et al. 2004. STAT3 is constitutively activated and supports cell survival in association with survivin expression in gastric cancer cells. *Oncogene*. 23(28):4921–4929. DOI: 10.1038/SJ.ONC.1207606.
23. Liang, D., Wang, Q., Zhang, W., Tang, H., Song, C., Yan, Z., Liang, Y. & Wang, H. 2024. JAK/STAT in leukemia: a clinical update. *Molecular Cancer*. 23(1):1–12. DOI: 10.1186/S12943-023-01929-1/TABLES/4.
24. Lim, C.P. & Cao, X. 2006. Structure, function, and regulation of STAT proteins. *Molecular bioSystems*. 2(11):536–550. DOI: 10.1039/B606246F.
25. Liu, K.D., Gaffen, S.L. & Goldsmith, M.A. 1998. JAK/STAT signaling by cytokine receptors. *Current Opinion in Immunology*. 10(3):271–278. DOI: 10.1016/S0952-7915(98)80165-9.
26. Michels, S., Trautmann, M., Sievers, E., Kindler, D., Huss, S., Renner, M., Friedrichs, N., Kirfel, J., et al. 2013. SRC signaling is crucial in the growth of synovial sarcoma cells. *Cancer research*. 73(8):2518–2528. DOI: 10.1158/0008-5472.CAN-12-3023.
27. Murray, P.J. 2007. The JAK-STAT signaling pathway: input and output integration. *Journal of immunology (Baltimore, Md.: 1950)*. 178(5):2623–2629. DOI: 10.4049/JIMMUNOL.178.5.2623.
28. Nagaraj, N.S., Washington, M.K. & Merchant, N.B. 2011. Combined blockade of Src kinase and epidermal growth factor receptor with gemcitabine overcomes STAT3-mediated resistance of inhibition of pancreatic tumor growth. *Clinical cancer research : an official journal of the American Association for Cancer Research*. 17(3):483–493. DOI: 10.1158/1078-0432.CCR-10-1670.

29. Neuwirt, H., Puhr, M., Santer, F.R., Susani, M., Doppler, W., Marcias, G., Rauch, V., Brugger, M., et al. 2009. Suppressor of Cytokine Signaling (SOCS)-1 Is Expressed in Human Prostate Cancer and Exerts Growth-Inhibitory Function through Down-Regulation of Cyclins and Cyclin-Dependent Kinases. *The American Journal of Pathology*. 174(5):1921–1930. DOI: 10.2353/AJPATH.2009.080751.
30. Qian, J., Xue, X. & Shannon, J. (in press). Characteristics of adverse event reporting of Xeljanz/Xeljanz XR, Olumiant, and Rinvoq to the US Food and Drug Administration. *Journal of Managed Care & Specialty Pharmacy*. 28(9):10.18553/jmcp.2022.28.9.1046. DOI: 10.18553/JMCP.2022.28.9.1046.
31. Ren, Y., Xu, R., Wang, Y., Su, L. & Su, J. 2025. Global, regional, and national burden of ovarian cancer in women aged 45 + from 1990 to 2021 and projections for 2050: a systematic analysis based on the 2021 global burden of disease study. *Journal of Cancer Research and Clinical Oncology*. 151(8):225. DOI: 10.1007/S00432-025-06277-9.
32. Roth, C.M. 2005. Molecular and cellular barriers limiting the effectiveness of antisense oligonucleotides. *Biophysical Journal*. 89(4):2286–2295. DOI: 10.1529/biophysj.104.054080.
33. Schust, J., Sperl, B., Hollis, A., Mayer, T.U. & Berg, T. 2006. Stattic: A Small-Molecule Inhibitor of STAT3 Activation and Dimerization. *Chemistry and Biology*. 13(11):1235–1242. DOI: 10.1016/j.chembiol.2006.09.018.
34. Sen, M., Tosca, P.J., Zwayer, C., Ryan, M.J., Johnson, J.D., Knostman, K.A.B., Giclas, P.C., Peggins, J.O., et al. 2009. Lack of toxicity of a STAT3 decoy oligonucleotide. *Cancer chemotherapy and pharmacology*. 63(6):983–995. DOI: 10.1007/S00280-008-0823-6.
35. Sen, M., Thomas, S.M., Kim, S., Yeh, J.I., Ferris, R.L., Johnson, J.T., Duvvuri, U., Lee, J., et al. 2012. First-in-human trial of a STAT3 decoy oligonucleotide in head and neck tumors: implications for cancer therapy. *Cancer discovery*. 2(8):694. DOI: 10.1158/2159-8290.CD-12-0191.
36. Shirogane, T., Fukada, T., Muller, J.M.M., Shima, D.T., Hibi, M. & Hirano, T. 1999. Synergistic roles for Pim-1 and c-Myc in STAT3-mediated cell cycle progression and antiapoptosis. *Immunity*. 11(6):709–719. DOI: 10.1016/S1074-7613(00)80145-4.
37. Souissi, I., Najjar, I., Ah-Koon, L., Schischmanoff, P.O., Lesage, D., Le Coquil, S., Roger, C., Dusanter-Fourt, I., et al. 2011. A STAT3-decoy oligonucleotide induces

cell death in a human colorectal carcinoma cell line by blocking nuclear transfer of STAT3 and STAT3-bound NF-κB. *BMC cell biology*. 12. DOI: 10.1186/1471-2121-12-14.

38. *STAT3 protein expression summary - The Human Protein Atlas*. n.d. Available: https://www.proteinatlas.org/ENSG00000168610-STAT3 [2025, June 27].
39. Strehlow, I. & Schindler, C. 1998. Amino-terminal signal transducer and activator of transcription (STAT) domains regulate nuclear translocation and STAT deactivation. *Journal of Biological Chemistry*. 273(43):28049–28056. DOI: 10.1074/jbc.273.43.28049.
40. Tamiya, T., Kashiwagi, I., Takahashi, R., Yasukawa, H. & Yoshimura, A. 2011. Suppressors of Cytokine Signaling (SOCS) Proteins and JAK/STAT Pathways. *Arteriosclerosis, Thrombosis, and Vascular Biology*. 31(5):980–985. DOI: 10.1161/ATVBAHA.110.207464.
41. Tang, X., Sui, X. & Liu, Y. 2023. Immune checkpoint PTPN2 predicts prognosis and immunotherapy response in human cancers. *Heliyon*. 9(1). DOI: 10.1016/j.heliyon.2023.e12873.
42. Thibault, T., Degrouard, J., Baril, P., Pichon, C., Midoux, P. & Malinge, J.M. 2017. Production of DNA minicircles less than 250 base pairs through a novel concentrated DNA circularization assay enabling minicircle design with NF-κB inhibition activity. *Nucleic acids research*. 45(5). DOI: 10.1093/NAR/GKW1034.
43. Timofeeva, O.A., Chasovskikh, S., Lonskaya, I., Tarasova, N.I., Khavrutskii, L., Tarasov, S.G., Zhang, X., Korostyshevskiy, V.R., et al. 2012. Mechanisms of unphosphorylated STAT3 transcription factor binding to DNA. *Journal of Biological Chemistry*. 287(17):14192–14200. DOI: 10.1074/jbc.M111.323899.
44. Turkson, J., Ryan, D., Kim, J.S., Zhang, Y., Chen, Z., Haura, E., Laudano, A., Sebti, S., et al. 2001. Phosphotyrosyl Peptides Block Stat3-mediated DNA Binding Activity, Gene Regulation, and Cell Transformation. *Journal of Biological Chemistry*. 276(48):45443–45455. DOI: 10.1074/jbc.M107527200.
45. Vasilescu, A.-G., Vasilescu, A.-M., Sima, L.E., Baran, N. & Szedlacsek, Ștefan-E. 2025. Breaking the cancer code: a novel DNA minicircle to disable STAT3 in ovarian cancer cells SKOV3. *Frontiers in Pharmacology*. 16. DOI: 10.3389/fphar.2025.1673427.
46. Verstovsek, S., Mesa, R.A., Gotlib, J., Levy, R.S., Gupta, V., DiPersio, J.F., Catalano, J. V., Deininger, M., et al. 2012. A Double-Blind, Placebo-Controlled Trial

of Ruxolitinib for Myelofibrosis. *New England Journal of Medicine*. 366(9):799–807. DOI: 10.1056/NEJMOA1110557.

47. Wu, C.J., Sundararajan, V., Sheu, B.C., Huang, R.Y.J. & Wei, L.H. 2019. Activation of STAT3 and STAT5 Signaling in Epithelial Ovarian Cancer Progression: Mechanism and Therapeutic Opportunity. *Cancers*. 12(1):24. DOI: 10.3390/CANCERS12010024.
48. Yang, E., Wen, Z., Haspel, R.L., Zhang, J.J. & Darnell, J.E. 1999. The linker domain of Stat1 is required for gamma interferon-driven transcription. *Molecular and cellular biology*. 19(7):5106–5112. DOI: 10.1128/MCB.19.7.5106.
49. Yang, E., Lerner, L., Besser, D. & Darnell, J.E. 2003. Independent and cooperative activation of chromosomal c-fos promoter by STAT3. *Journal of Biological Chemistry*. 278(18):15794–15799. DOI: 10.1074/jbc.M213073200.
50. Yang, J., Kunimoto, H., Katayama, B., Zhao, H., Shiromizu, T., Wang, L., Ozawa, T., Tomonaga, T., et al. 2020. Phospho-Ser727 triggers a multistep inactivation of STAT3 by rapid dissociation of pY705–SH2 through C-terminal tail modulation. *International Immunology*. 32(2):73–88. DOI: 10.1093/INTIMM/DXZ061.
51. Yue, P., Zhang, X., Paladino, D., Sengupta, B., Ahmad, S., Holloway, R.W., Ingersoll, S.B. & Turkson, J. 2012. Hyperactive EGF receptor, Jaks and Stat3 signaling promote enhanced colony-forming ability, motility and migration of cisplatin-resistant ovarian cancer cells. *Oncogene*. 31(18):2309–2322. DOI: 10.1038/ONC.2011.409.
52. Zhang, H., Li, H.S. & Watowich, S.S. 2016. Jak-STAT Signaling Pathways. *Encyclopedia of Immunobiology*. 3:134–145. DOI: 10.1016/B978-0-12-374279-7.11015-X.
53. Zhang, Q.Y., Ding, W., Mo, J.S., Ou-yang, S.M., Lin, Z.Y., Peng, K.R., Liu, G.P., Lu, J.J., et al. 2024. Novel STAT3 oligonucleotide compounds suppress tumor growth and overcome the acquired resistance to sorafenib in hepatocellular carcinoma. *Acta Pharmacologica Sinica*. 45(8):1701–1714. DOI: 10.1038/S41401-024-01261-4.
54. Zhang, X., Zhang, J., Wang, L., Wei, H. & Tian, Z. 2007. Therapeutic effects of STAT3 decoy oligodeoxynucleotide on human lung cancer in xenograft mice. *BMC Cancer*. 7(1):1–11. DOI: 10.1186/1471-2407-7-149/FIGURES/5.